



ELSEVIER

Physica C 366 (2002) 117–122

PHYSICA C

www.elsevier.com/locate/physc

# Relaxation of the transport critical current in deoxygenated $\text{YBa}_2\text{Cu}_3\text{O}_{7-\delta}$

R. Cobas<sup>a</sup>, A.J. Batista-Leyva<sup>a,b</sup>, S. García<sup>a,\*</sup>, E. Altshuler<sup>a</sup>

<sup>a</sup> *IMRE-Faculty of Physics, Superconductivity Laboratory, University of Havana, 10400, La Habana, Cuba*

<sup>b</sup> *Faculty of Engineering, Department of Physics, University of Holguín, 80100 Holguín, Cuba*

Received 22 January 2001; received in revised form 10 April 2001; accepted 13 May 2001

## Abstract

We present a study of the transport critical current relaxation for a set of carefully deoxygenated  $\text{YBa}_2\text{Cu}_3\text{O}_{7-\delta}$  polycrystalline samples, in such a way that the oxygen losses mostly come from the intergrain region, while the grains remain essentially unchanged. The dependence of the relaxation rates on the maximum magnetic fields applied to the sample, in the remanent state, is consistent with the predictions of a phenomenological model, in which the thermally activated relaxation of the intragrain magnetization provokes a time decay of the intergrain local fields, thus producing a temporal increase of the transport critical current. © 2002 Elsevier Science B.V. All rights reserved.

*Keywords:* Critical currents; Polycrystals;  $\text{YBa}_2\text{Cu}_3\text{O}_{7-\delta}$ ; Flux creep

## 1. Introduction

The study of the relaxation of the magnetization in the high- $T_c$  superconducting oxides is a frequent and useful approach to characterize the vortex dynamics (particularly flux creep effects), and the role of different types of structural defects as pinning centers. However, the time evolution of the transport critical current  $I_c$ , which is closely connected with the flux creep of the intragrain magnetization in polycrystals, has received by itself much less attention [1,2]. It is commonly ac-

cepted that the relaxation of the flux trapped in the grains changes the effective magnetic field at the weak links connecting them, thus influencing the transport current through the sample [3,4]. A systematic study of the time variation of  $I_c$  can be conducted by measuring the voltage at the critical current, after applying a given magnetic history to a properly chosen set of samples. Recently, we found that the transport critical current in polycrystalline high- $T_c$ s increases logarithmically in time, while the relaxation rate dependence on the maximum applied field  $H_m$  shows a broad maximum at low fields [5]. Although these results were reasonably described by a phenomenological model in that work, further analysis is needed to understand the peculiar behavior of relaxation rate with the magnetic history. In the present paper, we study the time evolution of the transport critical current  $I_c$ , in a set of carefully deoxygenated

\* Corresponding author. Address: Centro Brasileiro de Pesquisas Físicas (CBPF), Rua Xavier Sigaud 150, DME, 2 andar, Urca, CEP-22219-018 Rio de Janeiro, Brazil.

E-mail addresses: sgg@cbpf.br, supercon@imre.oc.uh.cu, jea@infomed.sld.cu (S. García).

polycrystalline samples of the system  $\text{YBa}_2\text{-Cu}_3\text{O}_{7-\delta}$ , in such a way that the oxygen losses mostly come from the intergrain region, while the grains remain essentially unchanged. Our measurements were performed using a PI controller, which allows us to collect thousands of values of  $I_c$  per hour. The aim is to characterize the  $I_c$  relaxation behavior, and its relation with the magnetic history, in samples with the same microstructure but with weak-link networks of different quality, looking for a comprehensive description of this process in bulk samples.

## 2. Experimental

$\text{YBa}_2\text{Cu}_3\text{O}_{7-\delta}$  samples were obtained by a standard solid-state reaction method. Stoichiometric amounts of high purity  $\text{Y}_2\text{O}_3$ ,  $\text{BaCO}_3$  and  $\text{CuO}$  were well mixed and pressed into pellets. The samples were sintered at  $950^\circ\text{C}$  for 16 h and slowly cooled ( $1^\circ\text{C}/\text{min}$ ) down to room temperature in an oxygen flow. Three intermediate treatments at  $900^\circ\text{C}$ ,  $920^\circ\text{C}$  and  $940^\circ\text{C}$  for 16 h each were performed, followed by fine crushing. A bar of approximately  $10 \times 1 \times 1 \text{ mm}^3$  was cut from one of the pellets.

The sample in as-sintered conditions will be referred as  $A_1$ . Once the transport measurements were performed, the  $A_1$  bar was introduced for 5 min in a long tubular furnace, previously stabilized at  $300^\circ\text{C}$  in air, (i.e., placed in the temperature plateau of the open furnace) and then quenched to room temperature. The resulting sample is denoted by  $A_2$ . After a new set of measurements, the  $A_2$  bar was annealed in air at  $300^\circ\text{C}$  for 25 min as described above and quenched to room temperature; this new sample is called  $A_3$ . The selection of this temperature and of the short annealing times is discussed below. Isothermal thermogravimetric (TG) measurements at  $300^\circ\text{C}$  in air were performed with a heating rate of  $10^\circ\text{C}/\text{min}$ , until the preset temperature is reached.

The resistive transition was measured by the four probe method using silver painted contacts. A bias ac current of 1 mA at a frequency of 80 Hz was applied through the outer pads, while the voltage across the inner ones was measured with a

lock-in amplifier with a maximum noise of 50 nV. The temperature was dynamically controlled with a resolution of  $\pm 0.02 \text{ K}$ .

The critical measurements were performed with a special PI pulsed-current set-up [6]. A sequence of alternate current pulses were injected to the sample in such a way that the PI system dynamically adjusted the height of the pulses in order to keep a constant dissipation of  $1 \mu\text{V}$  (taken as the voltage criterion to define  $I_c$ ). The voltage was sampled only at the plateau of each current pulse. In this way,  $I_c$  at any applied magnetic field, temperature or time was automatically measured just by reading the corresponding bias current. The magnetic field, generated by a long copper solenoid, was oriented perpendicular to the applied current. The maximum field used was  $H_m = 500 \text{ Oe}$  with an error of  $\pm 0.3 \text{ Oe}$ .

The  $I_c$  measurements were performed for different  $H_m$  values after the complete removal of the applied field. Once any previous magnetic history of the sample was erased by increasing the temperature up to  $1.3T_c$  at zero field, the temperature was stabilized to the chosen measurement value (85 K). The magnetic field was then increased at a rate of  $20 \text{ Oe/s}$  to the desired value of  $H_m$  and suppressed at the same rate. Special care was devoted to guarantee a true zero-field cooling of the sample, within the limitation imposed by the lack of shielding for the Earth's magnetic field. Then, the transport critical current was measured every second during 1 h, resulting in a  $I_c(H_m, t)$  vs  $t$  curve. The process was repeated for different values of  $H_m$ .

## 3. Results

The isothermal TG measurements at  $300^\circ\text{C}$  in air exhibit an initial flat region (including the heating interval), followed by a mass loss section which begins  $\sim 30 \text{ min}$  after the present temperature is attained. This loss gradually increases with time, until the curve levels off smoothly at an equilibrium value.  $A_1$ -type samples annealed in air for times inside the mass-loss interval exhibit severe changes in their resistivity curves. Fig. 1 shows the resistive transitions for samples  $A_1$ ,  $A_2$

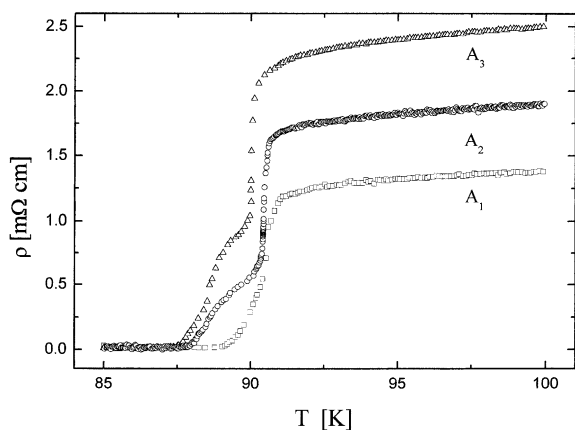


Fig. 1. Resistive transitions for  $\text{YBa}_2\text{Cu}_3\text{O}_{7-\delta}$  samples after heat treatments.  $A_1$ : sintered at  $950^\circ\text{C}$  in oxygen flow and slowly cooled;  $A_2$ :  $A_1 + 5$  min at  $300^\circ\text{C}$  for 25 min in air and quenched to room temperature.

and  $A_3$ . As can be verified, the normal-state resistivity regularly increases and the transitions become broader from  $A_1$  to  $A_3$ . The onset critical temperature,  $T_{\text{co}}$ , taken as the maximum of the derivative of the  $\rho(T)$  curves, is the same for  $A_1$  and  $A_2$  within the error of the measurements (90.76 and 90.75 K, respectively), while the zero-resistivity temperature,  $T_{\text{R}} = 0$ , is clearly lower for  $A_2$  (87.23 K) when compared to  $A_1$  (88.66 K). For  $A_3$ , both  $T_{\text{co}}$  and  $T_{\text{R}} = 0$  slightly diminish (90.13 and 87.19 K, respectively) relative to  $A_1$  and  $A_2$ .

The relaxation curves for all the samples ( $I_{\text{c}}(H_{\text{m}}, t)$  vs  $\log t$ ), measured at 85 K for some of the different applied values of  $H_{\text{m}}$ , follow the same behavior as the one of samples measured in Ref. [5]. We verified, through hysteresis measurements of  $I_{\text{c}}$  at low magnetic fields (known as “flux trapping curve” [5,7,8]), that the first critical field of the grains at 85 K in our samples is lower than 20 Oe being the same for samples  $A_1$  and  $A_2$  and slightly smaller for sample  $A_3$ ; so, in all these cases the grains were penetrated to different extents by the external field. As in Ref. [5], the linearity of the curves is remarkable, and the slope,  $S = dI_{\text{c}}/d(\log t)$ , gives the corresponding relaxation rates. Samples  $A_2$  and  $A_3$  have absolute values of  $I_{\text{c}}$  for a given  $H_{\text{m}}$  smaller than  $A_1$ .

Fig. 2 shows the dependence of  $S$  with  $H_{\text{m}}$  for the three studied samples. All of them shows a

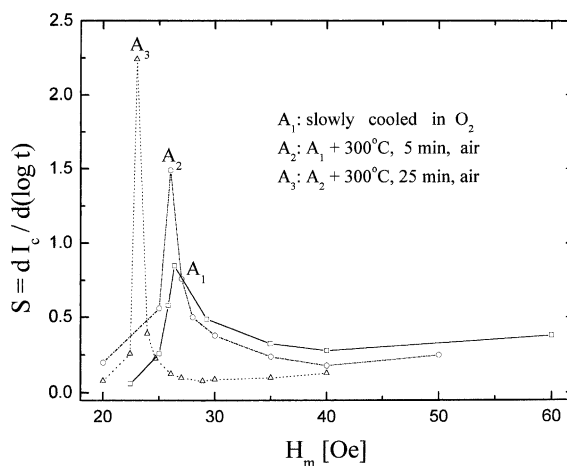


Fig. 2. Relaxation rates  $S = dI_{\text{c}}/d(\log t)$  for the  $\text{YBa}_2\text{Cu}_3\text{O}_{7-\delta}$  samples under study as a function of the maximum applied field  $H_{\text{m}}$  after complete removal. The lines are a guide the eyes.

maximum, which becomes more intense and narrow from  $A_1$  and  $A_2$  (26 Oe), while it is slightly displaced to a lower  $H_{\text{m}}$  value (23 Oe) for  $A_3$ . The high field region of the curves stabilizes at a level, which diminishes from  $A_1$  to  $A_3$ , i.e., the reverse behavior of the intensity of the corresponding maxima.

## 4. Discussion

### 4.1. Phenomenological model

In this section, we outline how to generate  $I_{\text{c}}$  curves as a function of the *effective* magnetic field,  $H_{\text{eff}}$ , at the intergrain junctions (i.e. not the *applied* field) for networks of different quality in their connectivity. This allows us a more clear interpretation of the  $I_{\text{c}}$  relaxation measurements in our samples, based on the phenomenological model reported in Ref. [5].

A widely accepted model to describe the behavior of the transport critical current  $I_{\text{c}}$  in a polycrystalline high- $T_{\text{c}}$  superconductor was early proposed by Peterson and Ekin [9]. The key idea is to consider the intergrain junctions embedded into an effective magnetic field  $H_{\text{eff}}$  resulting from the superposition of the external applied field and the one associated to the magnetization of the neighboring superconducting grains, which depends on

the magnetic history and time. Althshuler et al. [8] and Müller and Matthews [10] further extended the model, allowing the estimation of  $I_c$  at a given field after *any* magnetic history, assuming that the grains follow the Bean's critical state model [11]. The resulting  $I_c$  is then a function of the maximum applied field,  $H_m$ , the temperature,  $T$ , and the time elapsed since the magnetic field was suppressed,  $t$ , and can be written in its normalized form [5], as:

$$I_c(H_m, T, t) = I_c(T) \left| \frac{\text{Sen}(\pi H_{\text{eff}}(H_m, T, t)/H_0(T))}{\pi H_{\text{eff}}(H_m, T, t)/H_0(T)} \right|$$

if  $H_{\text{eff}} \leq H_0/2$  (1.1)

$$I_c(H_m, T, t) = I_c(T) \frac{H_0(T)}{\pi H_{\text{eff}}(H_m, T, t)}$$

if  $H_{\text{eff}} > H_0/2$  (1.2)

where  $H_0$  is the effective field value at which the first minimum appears in the  $I_c$  vs  $H$  “Fraunhofer” pattern of an *average* Josephson junction of the sample [12];  $I_c(T)$  is the temperature-dependent transport critical current at zero field.

Depending on the magnetic history of the sample,  $H_{\text{eff}}$  is described by different expressions [5,8,10], corresponding to different profiles of intragrain currents, according to the Bean's model. In this way,  $H_{\text{eff}}$  is expressed in terms of the full penetration field of the grains,  $H_g^*(T, t)$ , which allows us to introduce the time dependence in Eqs. (1.1) and (1.2). Taking into account that the original Anderson–Kim model cannot properly account for a various features of flux creep in high- $T_c$  superconductors, we use the so called *interpolation formula*, after Blatter et al. [13], for the time dependence of  $H_g^*(T, t)$ :

$$H_g^*(T, t) = H_g^*(0) \left( 1 + \mu \frac{K_B T}{U_0} \ln \left( \frac{t}{\tau} \right) \right)^{-1/\mu} \quad (1.3)$$

where  $H_g^*(0)$  is the average full penetration field of the grains at the initial instant and  $T = 0$ ,  $k_B$  is the Boltzmann's constant,  $U_0$  is the average pinning energy of the grains,  $\tau$  is a characteristic time of the order of  $10^{-6}$  s [14] and  $\mu$  ranges from 1/7 to 7/4, depending on the dimensionality of the pinning and creep regimes [15,16].

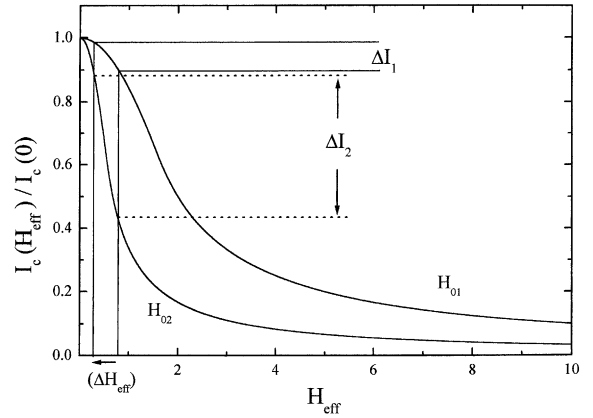


Fig. 3. Normalized  $I_c(H_{\text{eff}})/I_c(0)$  curves generated using Eqs. (1.1) and (1.2) (see text), for two weak-link networks with different characteristic fields  $H_0$  for an average junction ( $H_{01} > H_{02}$ ). The corresponding variations in the critical current  $\Delta I_1$  and  $\Delta H_{\text{eff}}$ , are indicated for each curve.

Fig. 3 shows two  $I_c(H_{\text{eff}})/I_c(0)$  curves generated using expressions 1.1 and 1.2 (for a constant temperature and a fixed time) with  $H_{01} > H_{02}$ , which will be used later on in the interpretation of our experimental results. We have  $U_0 = 0.6$  eV,  $H_g^*(0) = 90$  Oe and  $\mu = 1$  [5] in Eq. (1.3). A steeper decrease at low fields is obtained for the “weaker” network, represented by  $H_{02}$ , while the curve levels off more rapidly than that for  $H_{01}$  at higher  $H_{\text{eff}}$ . The introduction of a parameter as  $H_0$  is particularly convenient, because it allows to characterize the quality of the weak-link network as a whole.

#### 4.2. Analysis of the experimental curves

The increase in the normal-state resistivity values for samples A<sub>2</sub> and A<sub>3</sub>, along with the reduction in  $T_R = 0$  and the constancy in  $T_{co}$  (in addition to decrease of the absolute value of  $I_c$ ), indicate that the weak-link network is affected by the short-time annealing in air, while the grains remain unchanged. Since no decomposition of the YBCO matrix is observed, the mass loss must be due to oxygen release. Thus, we believe that the features of the resistivity curves for samples A<sub>2</sub> and A<sub>3</sub> are a signature of a very early stage of bulk deoxygenation (i.e., deoxygenation just at the junctions), which magnitude is beyond the sensitivity of our TG analyzer. The emergence of microcracks, due

to rapid warming and quenching, is possible. Both effects, oxygen deficiency and microcracks, lead to a degradation of the weak-link network. We note that, due to the low temperature and the short times of annealing, the original microstructure of  $A_1$  was preserved after the two thermal treatments; so, no changes in  $I_c$  are expected from variations in magnetic flux distribution in the link network. Thus, the relaxation of  $I_c$  is governed by the one of the grains magnetization, acting on a weakened intergrain network. In the light of the considerations presented in the previous section, the features of the  $S$  vs  $H_m$  curves should be described through the  $I_c$  dependence on  $H_{\text{eff}}$  displayed in Fig. 3. The curve for  $H_{01} > H_{02}$  is associated to the  $A_1$  sample.

For sample  $A_3$ , in addition to the increase in the normal-state resistivity and a broader transition, there was also observed a slight reduction in  $T_{\text{co}}$ , indicating that there begins the removal of some oxygen from the grains, promoted by the increase in the extension of the heat treatment. It is interesting to note that  $T_{R=0}$  diminishes to a lesser extent for  $A_3$  in comparison with the corresponding change between  $A_1$  and  $A_2$ , suggesting that the weakly bounded oxygen at the intergrain junctions was almost completely released after the 25 min annealing. We also included the analysis of the  $A_3$  sample, because it allows us to follow the regularities in the transport properties.

Once the external field is removed, an  $H_{\text{eff}}$  will be acting on the weak links, represented by an average junction of characteristic field  $H_0$ . This value of  $H_{\text{eff}}$  depends on the  $H_m$  reached in the particular experiments, and on the superconducting properties of the system. According to the corresponding slope in Fig. 3, this magnetic history determines the rate at which  $I_c$  will relax. Since the  $I_c(H_{\text{eff}})/I_c(0)$  vs  $H_{\text{eff}}$  dependence has an inflection point at low fields, the  $S$  vs  $H_m$  dependence will exhibit a maximum. This peak will be narrower for  $H_{02} < H_{01}$ , due to a more pronounced reduction in  $I_c$  for a weaker network. This is just the result obtained for sample  $A_2$ , as compared with  $A_1$ . It is worth to notice that, for both samples, a given value of  $H_m$  promotes the same  $H_{\text{eff}}$  since, as mentioned above, the oxygen content in the grains of these samples is essentially similar. Any possible

difference between the  $H_{\text{eff}}$  values for which the inflection points in the  $I_c(H_{\text{eff}})/I_c(0)$  curves occur are beyond the sensibility of our measurements. Furthermore, although the rate of change in  $H_{\text{eff}}$  due to the intragranular creep must be the same for both samples, the associated variation of the current in sample  $A_2$  ( $\Delta I_2$ ) near the inflection point, corresponding to a given reduction in  $H_{\text{eff}}$ , would be greater than that for sample  $A_1$  ( $\Delta I_1$ ), as indicated in Fig. 3; this implies  $dI_2/d(\log t) > dI_1/d(\log t)$ , resulting in a more intense peak for  $S$  in sample  $A_2$ , in agreement with Fig. 2.

As  $H_m$  increases,  $H_{\text{eff}}$  after field removal is higher than that for  $H_{02}$ . This means that the baseline of the  $S$  vs  $H_m$  curves at high fields should decrease as the intergrain transport properties are depleted, again in agreement with the behavior observed in our samples when going from  $A_1$  to  $A_3$ .

In the case of sample  $A_3$ , in addition to the effects of the deoxygenation treatments, on the intergrain connections, there are also small changes in the grain properties, as reflected by the slight reduction observed in  $T_{\text{co}}$ . Deoxygenation also reduces the value of the first critical field  $H_{\text{clg}}$ , as mentioned above. This implies that, for the same value of  $H_m$ , this sample will trap more flux than the  $A_1$  and  $A_2$  ones, thus giving a higher value of  $H_{\text{eff}}$  at the junctions. This means that the value of  $H_{\text{eff}}$  for the maximum relaxation rate in  $I_c$  (i.e., the inflection point in the corresponding  $I_c(H_{\text{eff}})/I_c(0)$  curve) would be reached for a lower  $H_m$  in comparison  $A_1$  and  $A_2$ , which is just the behavior detected, as shown in Fig. 3.

## 5. Conclusions

In this work, we have been able to tune, through careful deoxygenation treatments, the inter- and intragranular “quality” of a  $\text{YBa}_2\text{Cu}_3\text{O}_{7-\delta}$  polycrystal, without disturbing its microstructure, and to study the temporal relaxation of the transport critical current on the resulting set of samples. The results are coherent with the predictions of a phenomenological model in which the flux creep of the intragrain magnetization produces the decay of the intergrain effective field and, thus, a time increase of the transport critical current.

## Acknowledgements

We acknowledge L.E. Flores, C. Noda and C. Martínez for the design and setup of the measuring electronics. We also thank partial financial support from TWAS research grant no. 95-124 RG/PHYS/LA, and the University of Havana's "Alma Mater" Research Program. E. Altshuler acknowledges partial financial support from the WL Center for Pan-American Collaboration in Science and Technology.

## References

- [1] A.A. Zhukov, D.A. Komarkov, G. Karapetov, S.N. Gordev, R.I. Antonov, *Supercond. Sci. Technol.* 5 (1992) 338.
- [2] G. Ries, H.W. Neumüller, W. Schmidt, C. Struller, Proceedings of the 7th international Workshop on Critical Current in Superconductors, 24–27 January, 1994, Alpbach, Austria.
- [3] D.N. Matthews, G.J. Russell, K.N.R. Taylor, *Physica C* 171 (1990) 301.
- [4] E. Altshuler, J.L. González, *Physica C* 200 (1992) 195.
- [5] E. Altshuler, R. Cobas, A.J. Bastista-Leyva, C. Noda, L.E. Flores, C. Martínez, M.T.D. Orlando, *Phys. Rev. B* 60 (1999) 3673.
- [6] L.E. Flores, C. Martínez, *Cryogenics* 36 (1996) 705.
- [7] E. Altshuler, S. García, J. Barroso, *Physica C* 177 (1991) 61.
- [8] E. Altshuler, J. Musa, J. Barroso, A.R.R. Papa, V. Venegas, *Cryogenics* 33 (1993) 308.
- [9] R.L. Peterson, J.W. Ekin, *Phys. Rev. B* 637 (1988) 9848.
- [10] K.H. Müller, D.N. Matthews, *Physica C* 206 (1993) 207.
- [11] Ch. Bean, *Rev. Mod. Phys.* 30 (1964) 31.
- [12] A.R.R. Papa, E. Alshuler, *Solid State Commun.* 76 (1990) 799.
- [13] G. Blatter, M. Feigel'man, V.B. Geshkenbein, A.I. Larkin, M. Vinokur, *Rev. Mod. Phys.* 66 (1994) 1125.
- [14] Y. Yeshurun, A.P. Malozemoff, A. Shaulov, *Rev. Mod. Phys.* 68 (1996) 10510.
- [15] M.V. Feigel'man, V.B. Geshkenbein, A.I. Larkin, V.M. Vinokur, *Phys. Rev. Lett.* 62 (1989) 2303.
- [16] V.M. Vinokur, P.H. Kes, A.E. Koshelev, *Physica C* 168 (1990) 29.